URSI GASS 2021, Rome, Italy, 28 August - 4 September 2021

Modeling of energetic electron precipitation affected by oblique whistler mode chorus emissions in the outer radiation belt

Yi-Kai Hsieh*(1) and Yoshiharu Omura(1)
(1) Research Institute for Sustainable Humanosphere, Kyoto University, Japan

Abstract

Whistler mode wave-particle interaction is a significant mechanism causing energetic electron accelerations and pitch angle scatterings in the Earth's outer radiation belt. Interactions between parallel propagating whistler mode chorus waves and electrons have been studied for decades and people understand their physical processes well. While the oblique whistler mode wave-particle interactions are still not clear nowadays. In this study, we focus on how oblique whistler chorus emissions cause energetic electron precipitation (EEP), and what are the differences between the precipitation process affected by parallel propagating chorus emissions and that by oblique propagating chorus emissions. We apply Green's function method and its convolution integrals to trace the evolution of energetic electron fluxes around L=4.5 field lines for about 1000 consecutive chorus emissions. To built a Green's function set, 183,600,000 electrons with energies from 10 keV to 6 MeV and equatorial pitch angles from 5°to 89° are inputted in a test particle simulation. We compare the precipitation phenomena among 3 wave models for different wave normal angles. The results show that oblique chorus emissions lead to more electron precipitation than that led by parallel chorus emissions. Multiple resonance effect in the oblique whistler mode wave-particle interactions are the crucial reason for the greater precipitation.

1 Introduction

Energetic electron precipitation (EEP) for a wide energy range has been observed in good collaboration with whistler mode chorus emissions in the Earth's outer radiation belt [e.g., 1]. *Hikishima et al.* [2] performed a one-to-one correspondence between the electron microbursts and the generation of parallel discrete chorus elements for 10–100 keV electrons by self-consistent particle-in-cell simulation. Nonlinear trapping via Landau resonance in the oblique whistler mode wave-particle scatters energetic electrons to lower pitch angles effectively. However, so far there is no study verifying the relation between EEP and oblique chorus emissions. In this study, we check if chorus emissions can cause EEP for wide electron energy ranges by test particle simulations in a 3-D dipole magnetic field for both parallel propagating chorus emissions and obliquely propagating chorus emissions. We further apply Green's function method and its convolution integrals to trace long-time evolution of the electron precipitation with consecutive chorus emissions. Using the simulation results, we compare the electron precipitation by purely parallel chorus emissions and that by oblique chorus emissions. Moreover, we introduce a new process of electron precipitation by multiple resonance effect in the oblique whistler mode wave-particle interactions.

2 Simulation Method

2.1 Test Particle Simulation

We apply test particle simulations to reproduce wave-particle interactions between lower-band chorus emissions and energetic electrons in the outer radiation belt. The background magnetic field is a 3-D dipole field. We utilize the Bumeman-Boris method to integrate the equations of motions of electrons given by

$$\frac{d(m\mathbf{v})}{dt} = q\left(\mathbf{E} + \mathbf{v} \times \mathbf{B}\right), \tag{1}$$

$$\frac{d\mathbf{x}}{dt} = \mathbf{v}. \tag{2}$$

Parameters inputted in simulations are listed in Table 1. For waves, we assume that a pair of lower-band chorus emissions are generated at the equator and then propagate to higher latitudes in both northward and southward directions. Three whistler mode wave models with different wave normal angles θ are used in the test particle simulations. Those are one purely parallel propagating chorus emissions (Case 1) and two obliquely propagating chorus emissions (Case 2 & 3). The wave normal angles as functions of latitude (*Lat*) for Case 2 and 3 are shown in Figure 1. We employed subpacket structures in wave amplitude (see Figure 2b) and rising-tone frequency for the emissions. We localize the longitudinal chorus occur region from $\Phi = 0°$ to $\Phi = 60°$.

2.2 Green's Function Method & Convolution Integral

Omura et al. [3] introduced the numerical Green's function method and convolution integral method to trace energetic

Table 1. Parameters used in simulations

Parameters		Normalized	Real
L-shell	L		4.5
Background magnetic field (Eq)	B_{eq}		342 nT
Electron gyrofrequency (Eq)	Ω_{eq}		9.58 kHz
Electron plasma frequency	ω_{pe}	4 Ω_{eq}	38.3 kHz
Cold electron density	n_e		17/cc
Source electron density	n_h	0.005 n_e	0.0865/cc
Wave frequency (Min)	ω	0.25 Ω_{eq}	2.39kHz
Wave frequency (Max)	ω	0.5 Ω_{eq}	4.79kHz

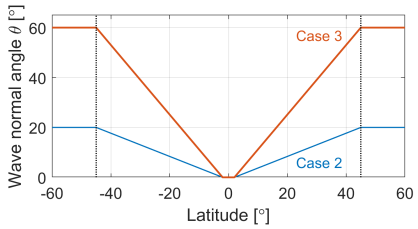

Figure 1. Wave normal angles θ for Case 2 (blue line) and Case 3 (orange line) as functions of latitude. Within $|Lat| < 2°$, $\theta = 0°$ for both cases. Within $2° < |Lat| < 45°$, θ are linear functions. For $|Lat| > 45°$, the θ are constants $\theta_{max} = 20°$ and $60°$ for Case 2 and Case 3, respectively.

electron distribution functions after interaction with target waves. *Kubota and Omura* [4] extended the method by adding the electron longitudinal information in the Green's functions. The method assumes a delta function in the phase space of kinetic energy K, equatorial pitch angle α, and longitudinal position Φ as the initial electron distribution function, and then we obtain a new distribution function after interaction with the target wave. The new distribution function is the Green's function $G(K, K_0, \alpha, \alpha_0, \Phi, \Phi_0)$. A Green's function is treated as a result of one cycle of chorus wave-particle interaction. We build up a set of Green's function by demonstrating test particle simulations for electron K ranges from 10 keV to 6 MeV with an interval 10 keV, α ranges from 5° to 89° with an interval 1°, and Φ ranges from 0° to 360° with an interval 10°. Notice that our target L value is 4.5, so the equatorial loss cone angle α_{loss} is 4.56° corresponding to an altitude of 100 km from the Earth's surface. For an initial delta function, 3,600 electrons with random gyrophases and latitudes are used. The total number of electrons for generating a Green's function set is $183,600,000$.

To reproduce the wave-particle interactions for consecutive chorus emissions, the first step is to set an initial electron distribution function and then obtain a new distribution function by applying a Green's function set. The second step is to regard the new distribution function as new initial distribution, and then apply the Green's function again for the next distribution function. By repeating the steps m times, we can simulate the results of wave-particle interactions of m successive emissions without calculating the test particle simulation for m emissions, whose simulation costs a lot of computation resources. This process is so-called convolution integral.

3 Results

3.1 Process of Pitch Angle Scattering

We first examine the results of the test particle interactions. Figure 2 shows 4 examples for electrons starting at $K = 50$ keV and $\alpha = 20°$ in Case 3. Figure 2a plots electron trajectories in a Lat–$v_{\parallel}$ (latitude–electron parallel velocity) phase space. Figure 2b is electron trajectories and spatiotemporal profile of generation and propagation of chorus wave amplitude. The red and blue curves represent resonance velocities of $n = 1$ cyclotron resonance and $n = 0$ Landau resonance, respectively. The resonance velocities are given by

$$V_R^{(n)} = \frac{1}{k_{\parallel}} \left(\omega - \frac{n\Omega_e}{\gamma} \right), \tag{3}$$

where n is the harmonic number, $k_{\parallel}$ is parallel wave number, Ω_e is local electron gyrofrequency, and γ is the Lorentz factor. The dotted lines stand for $\omega = 0.25\Omega_{eq}$ and the dashed lines denote $\omega = 0.5\Omega_{eq}$. Note that electrons interact with chorus emissions when the parallel velocity $v_{\parallel}$ moving close to the resonance velocity. Hence, we can recognize that an electron is affected by a certain resonance in Figure 2a. In Figure 2b we can know the timing of electrons undergoing resonances and make sure the electrons are inside the wave subpackets. There are two main processes in the whistler mode wave-particle interactions. One is the untrapped resonance process, which makes an electron energy slightly smaller and lowers the α of the electron. The other is the nonlinear trapping process, which makes effective energy gain of the resonant electrons. Figure 2c shows the time series of kinetic energies, which helps us to verify the resonance processes. Figure 2d denotes the time series of equatorial pitch angles α. The green curve drops to the loss cone, which is shown as the gray area, around time=320 ms (red area). This electron is a untrapped resonance particle for $n = 1$ cyclotron resonance. Most of the precipitate electrons undergo this process. The yellow curve undergoes two nonlinear trapping processes. The first one is the $n = 1$ cyclotron resonance (~165–250 ms) and the second one is the $n = 0$ Landau resonance (~250–380 ms). Both resonances make effective accelerations but the different tendencies of pitch angle scattering. The first one makes higher α and the second one leads to lower α. The black curve is also affected by 2 resonances. Around 280 ms (green area) the electron drops close to the loss cone by untrapped resonance process of the $n = 1$ resonance, and then at around 500 ms (blue area) it is pushed into the loss cone by the nonlinear trapping of the $n = 0$ Landau resonance. Here we find that Landau resonance can directly cause electron precipitation. However, this kind of precipitation by Landau resonance is rare and it requires an electron already close to the loss cone. The purple curve first undergoes $n = 1$ untrapped resonance process and then undergoes a long $n = 0$ nonlinear trapping. Nonetheless, the nonlinear trapping via

the $n = 0$ Landau resonance is not able to scatter the electron into the loss cone.

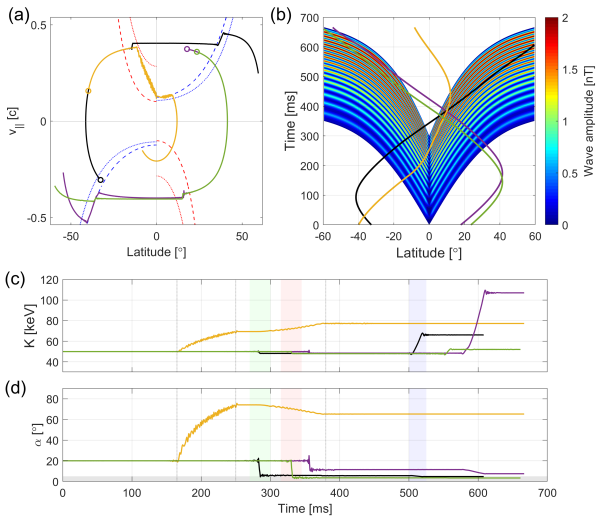

Figure 2. (a) Electron trajectories in a latitude–electron parallel velocity phase space. (b) Electron trajectories and spatiotemporal profile of chorus wave amplitude for Case 3 with subpacket structure. (c) Time series of kinetic energy variations. (d) Time series of equatorial pitch angle variations.

3.2 Results of Convolution Integrals

We set an initial electron distribution function F_{0EQ} as a stationary equatorial distribution function with uniform K from 10 to 30 keV and uniform α from 5° to 89°. The initial distribution is treated as source electrons generating the waves. We also assume an incessant influx of source electrons from the Earth's tail into the inner magnetosphere. Thereby, we keep the F_{0EQ} as a constant distribution during all cycles of chorus interactions. We apply the convolution integral method described in 2.2 to the initial distribution function. Figure 3 shows the equatorial distribution functions F_{mEQ} integrated over the longitudinal direction with interaction cycle m = (a) 20, (b) 50, (c) 600, and (d)1000. These integrals of F_{0EQ} over K, α, and Φ are normalized to $1m^{-2}$. The dark green and magenta curves represent the distribution functions integrated over α below and above α_{loss} as functions of K, respectively. It is obvious that after more cycles of interactions, both precipitation and acceleration increased. In Figure 3a we find that electrons are accelerated to MeV level rapidly in Case 3, and in Figure 3c we have electron more than 4 MeV in Case 1. According to the dark green curves, we conclude that chorus emissions contribution to energetic electron precipitation for a wide energy range from few tens of keV to a few MeV. However, the number of electrons precipitated into the loss cone in the energy range $K > 0.5$ MeV is much less than that of electrons being accelerated and remaining in the radiation belt.

We integrates the precipitation fluxes over K, α, Φ for each cycle m and plot them in Figure 4. Figure 4a–d compare the EEP among the 3 cases at different energy ranges, those are (a) $K < 100$ keV, (b) 100 $keV < K < 500$ keV, (c) 0.5 $MeV < K < 1$ MeV, and (d) $K > 1$ MeV. For all cases, most of the precipitation occurs in $K < 100$ keV. Furthermore, in each energy range, the precipitation affected by oblique chorus emissions are greater than those affected by parallel chorus emissions, and the electron precipitation ratio (oblique case/parallel case) becomes larger for greater electron energies. At $K < 100keV$, it is interesting that precipitation in Case 2 is greater than that in Case 3, indicating that we cannot conclude that larger wave normal angles cause more precipitation.

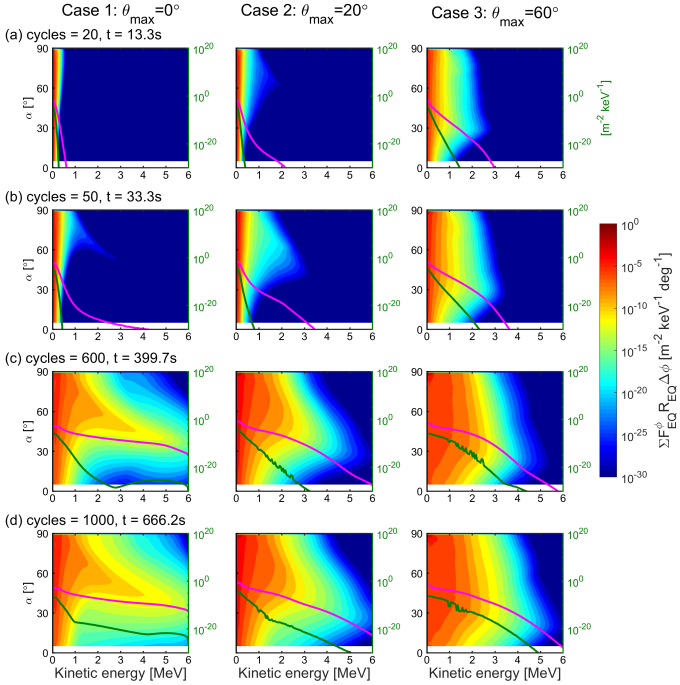

Figure 3. (a–d) Time evolution of the equatorial electron distribution functions $F^{\Phi}_{mEQ}(E, \alpha, \Phi)$ integrated over the longitudinal direction after m cycles of interactions with parallel chorus emissions (left column) or with oblique chorus emissions (middle and right columns). The dark green and magenta curves represent the distribution functions integrated over α below and above α_{loss} as functions of K, respectively.

4 Discussion

In oblique whistler mode wave-particle interactions, an electron can go through not only $n = 1$ cyclotron resonance but also the $n = 0$ Landau resonance and higher-order resonances during a bounce motion, indicating that the electron has more opportunities to move toward a lower equatorial pitch angle. The $n = 0$ Landau resonance can make high-α electrons move to lower α via the nonlinear trapping effectively. On the other hand, the $n = 1$ or $n = 2$ cyclotron can lower electron's α via the untrapped resonance process. Finally, after a few cycles of interactions, an electron moves close to α_{loss} and then be pushed into the loss cone by the

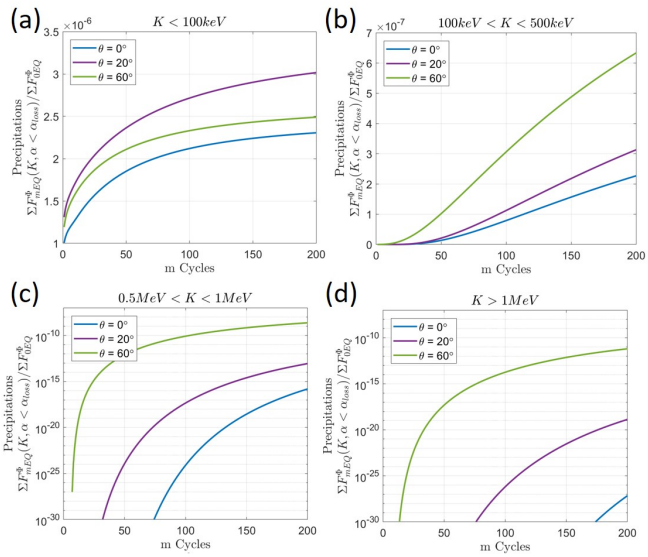

Figure 4. Electron precipitations for 3 Cases in different energy ranges. (a) $K < 100\ keV$, (b) $100\ keV < K < 500\ keV$, (c) $0.5\ MeV < K < 1\ MeV$, and (d) $K > 1\ MeV$.

$n = 1$ cyclotron resonance. A schematic picture explaining this process is plotted in Figure 5. The steps of the energetic electron precipitation for oblique whistler mode wave-particle interactions are: (1) A high-α electron obtains energy from a chorus emission and its α becomes lower via nonlinear trapping of Landau resonance. (2) The electron bounce back toward the equator and then is pushed into the loss cone via the untrapped resonance process of cyclotron resonance by another emission. (3) The electron precipitates in the opposite hemisphere.

Therefore, we conclude that the multiple resonance effect is the reason for more precipitation in the oblique whistler mode wave-particle interactions, and the precipitation process cannot be done by a single emission.

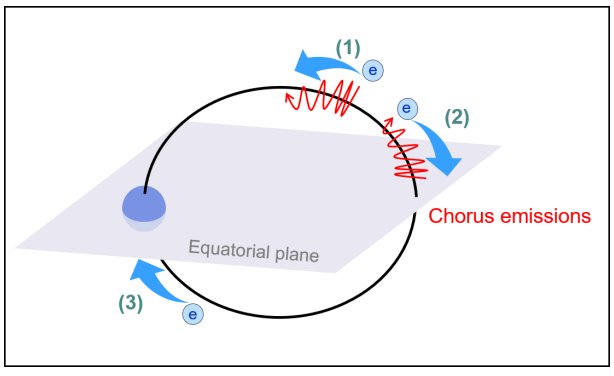

Figure 5. Schematic picture of the wave-particle interactions between chorus emissions and an electron showing the precipitation process by multiple resonances of different emissions at different locations. (1) A high-α electron gets energy and its α becomes lower via Landau resonance. (2) The electron is pushed into the loss cone via cyclotron resonance. (3) The electron precipitates.

5 Summary

Our findings in the test particle simulations are summarized as follows:

1. Most of the EEP events are less than $100keV$. We do find EEP for relativistic electrons but the fluxes are much smaller than those of electrons less than $100keV$.

2. Most of the EEP events are directly caused by the untrapped resonance process of the $n = 1$ cyclotron resonance.

3. Nonlinear trapping by n=0 Landau resonance also directly contributes to EEP, but the opportunity is much less than precipitation by the untrapped resonance process of the $n = 1$ cyclotron resonance.

4. Obliquely propagating chorus emissions affect more EEP than parallel propagating chorus emissions. Multiple resonance effect is the reason for the phenomenon.

6 Acknowledgements

Computations in the present study were performed on the KDK system of the Research Institute for Sustainable Humanosphere (RISH) at Kyoto University, Japan. This work was supported by MEXT/JSPS KAKENHI Grants 17H06140.

References

[1] Y. Miyoshi, S. Oyama, S. Saito, S. Kurita, H. Fujiwara, R. Kataoka, Y. Ebihara, C. Kletzing, G. Reeves, O. Santolik, M. Clilverd, C. J. Rodger, E. Turunen, and F. Tsuchiya, "Energetic electron precipitation associated with pulsating aurora: EISCAT and Van Allen Probe observations," *J. Geophys. Res. Space Physics*, **120**, 21 April 2015, pp. 2754—2766, doi:10.1002/2014JA020690.

[2] Hikishima, M., Y. Omura, and D. Summers, "Microburst precipitation of energetic electrons associated with chorus wave generation," *Geophys. Res. Lett.*, **37**, 7 April 2010, L07103, doi:10.1029/2010GL042678.

[3] Omura, Y., Y. Miyashita, M. Yoshikawa, D. Summers, M. Hikishima, Y. Ebihara, and Y. Kubota, "Formation process of relativistic electron flux through interaction with chorus emissions in the Earth's inner magnetosphere," *J. Geophys. Res. Space Physics*, **120**, 21 November 2015, pp. 9545–9562 doi:10.1002/2015JA021563.

[4] Kubota, Y., and Omura, Y. "Nonlinear dynamics of radiation belt electrons interacting with chorus emissions localized in longitude," *J. Geophys. Res. Space Physics*, **123**, 20 Jun 2018, pp. 4835–4857, doi:10.1029/2017JA025050.